Antibacterial efficacy studies of silver nanoparticles against *Escherichia coli* ATCC-15224

6.1. Introduction

Synthesis of nanosized drug particles with tailored physical and chemical properties are of great interest in the development of new pharmaceutical products [1]. Emergence of bacterial strains, resistant to current antibiotics has become a serious public health issue that raised the need to develop new bactericidal materials [2]. However, the phenomenon of enhanced biological activity and certain material changes resulting from nanoparticles is not yet understood fairly. Experimental investigations have shown encouraging results about the activity of different drugs and antimicrobial formulation in the form of nanoparticles. Activity of nanoemulsions of oil droplets against bacteria and spores has been analyzed [3].

Silver is a non-toxic, safe inorganic antibacterial agent being used for centuries and is capable of killing about 650 microorganisms that cause diseases [4]. Silver has been described as being 'oligodynamic', that is, its ions are capable of causing a bacteriostatic (growth inhibition) or even a bactericidal (antibacterial) impact. Therefore, it has the ability to exert a bactericidal effect at minute concentrations [5]. It has a significant potential for a wide range of biological applications such as antibacterial agents for antibiotic resistant bacteria, preventing infections, healing wounds and anti-inflammatory [6]. Silver ions (Ag^+) and its compounds are highly toxic to microorganisms exhibiting strong biocidal effects on many species of bacteria but have a low toxicity towards animal cells. Therefore, silver ions, being antibacterial component, are employed in formulation of dental resin composites, bone cement, ion exchange fibers and coatings for medical devices [7-8].

Bactericidal behavior of nanoparticles is attributed to the presence of electronic effects that are brought about as a result of changes in local electronic structures of the surfaces due to smaller sizes. These effects are considered to be contributing towards enhancement of reactivity of silver nanoparticles surfaces. Ionic silver strongly interacts with thiol groups of vital enzymes and inactivates them. It has been suggested that DNA loses its replication ability once the bacteria are treated with silver ions [9]. Two dimensional electrophoresis and

proteins identification analysis of antibacterial action of silver nanoparticles have disclosed accumulation of envelope proteins precursors. Silver nanoparticles destabilize plasma membrane potential and depletion of levels of intracellular adenosine triphosphate (ATP) by targeting bacterial membrane resulting in bacterial cell death [10].

Conventional compounds of silver such as silver nitrate and silver sulfadiazine are used to prevent bacterial growth in drinking water, sterilization and burn care. It is economical to consolidate silver in polymers, composites, fabrics and catheters for antibacterial functionality [11-14]. The present study was conducted to synthesize silver nanoparticles by inert gas condensation method and characterization of their crystalline structure, morphology, estimation of mean size and distribution by XRD and TEM techniques. Antibacterial activity of these silver nanoparticles as a function of nanoparticles concentration has been demonstrated for inhibiting the growth and killing of *Escherichia coli* (*E. coli)* ATCC-15224 strain in liquid as well as on solid growth media. The ultimate objective was to study the interaction between bacteria and silver nanoparticles to understand the bacterial inhibition mechanism.

6.2. Experimental setup

6.2.1. Synthesis of silver nanoparticles

IGC method described in section 3.2.1.1 of chapter 3 was followed to synthesize silver nanoparticles by metal evaporation in argon atmosphere. Pieces of 0.5 mm diameter bulk silver wire (Sigma Aldrich, 99.9 % pure) were placed in the molybdenum evaporation boat. IGC process chamber was evacuated to a base pressure of the order of 10^{-6} torr. Argon gas (99.99% pure) was introduced into the process chamber through a moisture trap at a pressure of 100 mtorr. The synthesized silver nanoparticles were characterized by XRD and TEM for estimation of crystalline structure, mean size and morphology, according to the procedures described in section 3.3.1, 3.3.3 of chapter 3.

6.2.2. Antibacterial test

Silver nanoparticles' bactericidal effect was studied against Gram-negative bacteria. These nanoparticles were dispersed in autoclaved deionized water by ultrasonication. Aqueous dispersions of silver nanoparticles of desired concentrations were made. An axenic culture of

E. coli ATCC- 15224 was grown in liquid nutrient broth medium CM-01 (Oxoide, England, Lab lemco powder 1 g, NaCl 5 g, peptone 5 g and yeast extract 2 g). For this experimental investigation, freshly grown bacterial inoculum (10^4 cells/ ml) of *E. coli* was incubated in the presence of a range of silver nanoparticles loadings of 0, 20, 40, 60, 80 and 100 μg/ml added in each flask to observe the bacterial cell growth pattern at 310K (37°C) and 150 rpm. Total solution volume used in each flask was 50 ml. In liquid medium, growth of *E. coli* was indexed by measuring optical density (OD). OD measurements on the samples collected from the solutions were carried out at λ_{max} 600 nm against growth media control by UV- Vis spectroscopy after every 2 hrs and up to 24 hrs. Control flasks were containing 50 ml of all the initial reaction components except the silver nanoparticles. Samples were collected for colony forming units (CFU) measurements on the solid medium. Samples treated with nanoparticles were spread on nutrient agar plates and after incubation at 37°C (310K) for 24 hours, the numbers of CFU were counted. Bacterial cells treated with nanoparticles were collected by centrifugation of liquid samples at 10,000 rpm for 10 minutes. SEM and TEM analyses on bacterial samples treated with silver nanoparticles were performed by following the procedure described in section 3.3.2 and 3.3.3 of chapter 3. All experiments were performed under sterile conditions and in triplicate.

6.3. Results

6.3.1. Characterization of silver nanoparticles

6.3.1.1 X-ray diffraction analysis of nanoparticles

XRD pattern of silver nanoparticles recorded by following the procedure described in section 3.3.1 of chapter 3, is shown in Figure 6.1. The analysis was carried out in 2θ range 20°-80°, with step size 0.05° in a Rigaku D-Max B diffractometer. All diffraction peaks correspond to the characteristic face centered cubic (FCC) silver lines. These diffraction lines observed at 2θ angle 38.1°, 44.3°, 64.4°, and 77.5° respectively, have been indexed as (111), (200), (220) and (311) respectively. XRD patterns were analyzed to determine peak intensity, position and width. Full-width at half-maximum (FWHM) data was used with the Scherrer formula explained in section 3.3.1 of chapter 3 [15]. The mean size of nanoparticles estimated by XRD is 15nm.

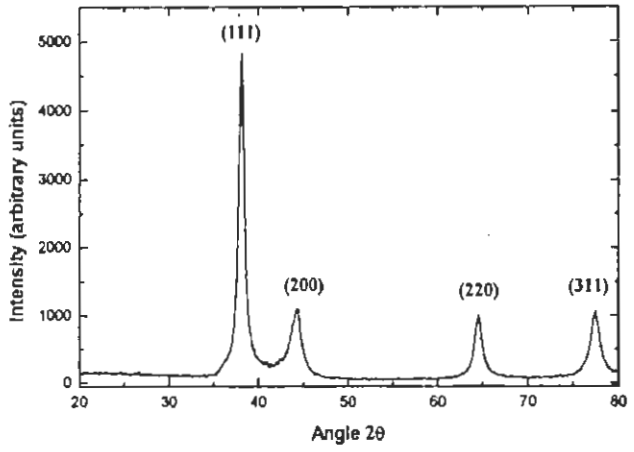

Figure 6.1: XRD pattern of silver nanoparticles synthesized by inert gas condensation method, used in this study

6.3.1.2. TEM analysis of nanoparticles

A representative TEM micrograph of silver nanoparticles is shown in Figure 6.2, which demonstrates agglomerated clusters of spherical shape and narrow particle size distribution. Nanoparticles formed in the gas phase synthesis processes follow lognormal distribution function (LNDF) [16-19]. The mean particle size estimated from the TEM was 16nm, which compared well with size estimated from XRD data.

Figure 6.2: TEM micrograph of silver nanoparticles synthesized by inert gas condensation method, used in this study

6.3.2 Antibacterial test

6.3.2.1. Optical density measurement

Silver nanoparticles were added in the liquid growth medium in the range of 0, 20, 40, 60, 80 and 100 μg/ ml at the beginning of bacterial cell growth. Number of bacteria cells (10^4 cells/ ml) added in each flask containing 50 ml of solution was closer to the real life situations. A control flask was containing 50 ml of all the initial reaction components of liquid growth medium except the silver nanoparticles. Optical densities as a function of time were measured periodically up to 24 hours of the control and the solutions containing different concentrations of silver nanoparticles are plotted and shown in Figure 6.3.

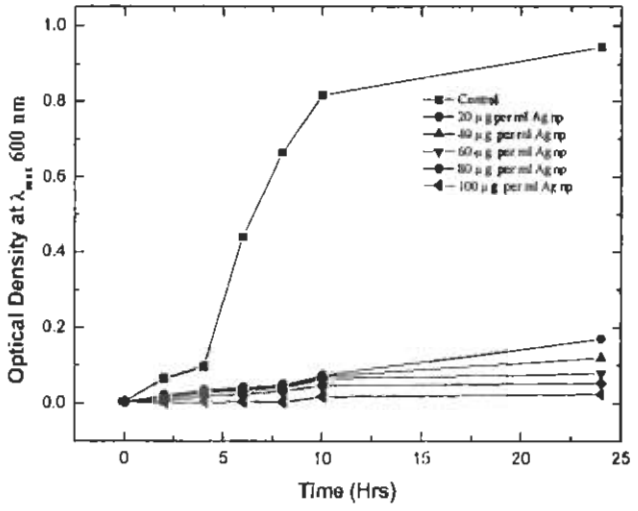

Figure 6.3: Optical density as a function of time for estimation of bacterial growth in solution studies

6.3.2.2. Estimation of colony forming units (CFU)

Bacterial cells treated with nanoparticles were spread on nutrient agar plates which were incubated at 37°C (310K) for 24 hrs, the number of colony forming units (CFU) was counted. Figure 6.4 shows the plot of number of bacterial colonies grown on nutrient agar plates as a function of concentration of silver nanoparticles. The numbers of CFU have been observed to reduce significantly with the increasing silver nanoparticles loadings.

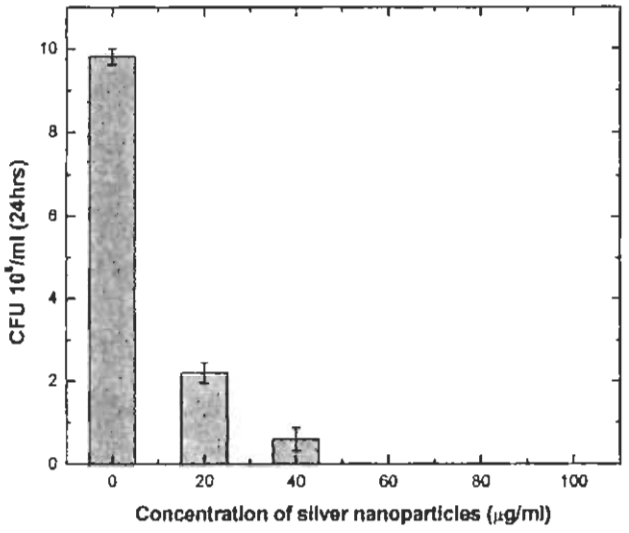

Figure 6.4: Antibacterial characterization by CFU as a function of silver nanoparticles concentration on agar plates

6.3.2.3. SEM analysis of particles-bacterial interaction

Silver nanoparticles adhered to the membrane of bacteria were observed by scanning electron microscopy. Figure 6.5a, shows the micrograph of bacterial cell biomass treated with silver nanoparticles in which silver has been found adhered to the bacterial cell wall surface. The presence of elemental silver on the bacterial cells was supported by EDS analysis that is shown in Figure 6.5b.

6.3.2.4. TEM analysis of particles-bacterial interaction

TEM micrograph shows silver nanoparticles not only adhered at the surface of cell membrane, but also penetrated inside the bacterial cells. Figure 6.6a shows micrograph in which silver nanoparticles were observed bound to the cell wall of bacteria. Figure 6.6b shows the micrograph in which nanoparticles were observed penetrated inside the bacterial cells.

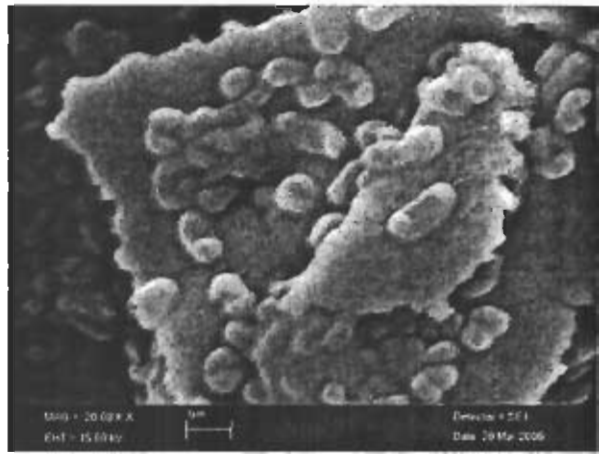

Figure: 6.5a

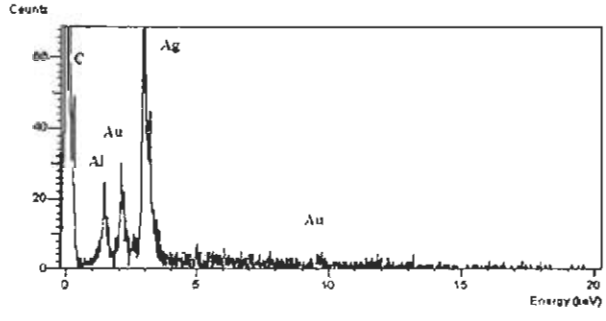

Figure: 6.5b

Figure 6.5: (a) SEM micrograph of *E. coli* treated with silver nanoparticles (b) EDS analysis

6.4. Discussion

Silver nanoparticles were dispersed in the autoclaved deionized water by ultrasonication so that soft agglomerates were broken down into smaller nanoparticles. Aqueous dispersions of these nanoparticles at desired concentrations were made. Number of bacteria cells (10^4 cells/ ml) added in each flask containing 50 ml of solution were considered closer to the real life situations. Shaking during incubation provided bacteria aeration and homogeneity. Control flasks containing all the initial reaction components except the silver nanoparticles showed no antibacterial activity. Bacterial cells grow by a process of binary fission in which one cell doubles in size and splits into halves to produce two identical daughter cells. Bacterial cell growth enhances the turbidity of the liquid nutrient medium, as a result optical absorption increases in the solution.

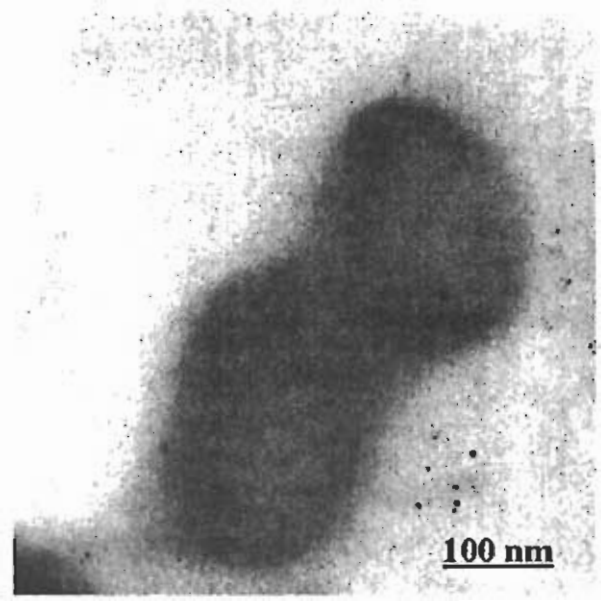

Figure: 6.6a

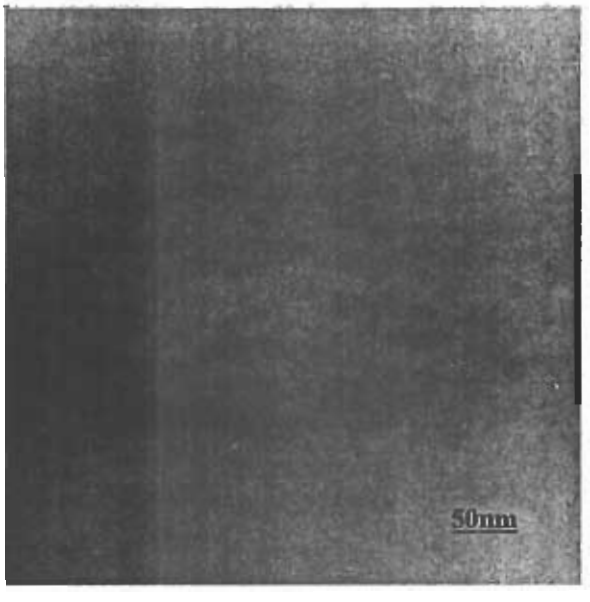

Figure: 6.6b

Figure 6.6: TEM micrograph (a) interaction of silver nanoparticles with *E. coli* (b) penetration of silver nanoparticles in *E. coli*

It has been observed from the OD plot given in Figure 6.3 that optical absorption in the growth medium decreased in comparison to the control with increasing concentration of silver nanoparticles. This has been attributed to the reduced growth of bacterial cells. Silver nanoparticles at concentrations of 20 μg/ ml and higher were found effective bactericides, but a complete bacterial growth inhibition has been witnessed at 60 μg/ ml and above. Because there was virtually no bacterial growth, as a result optical absorption was insignificant. The bacterial cell colonies on agar-plates were detected by viable cell counts. Viable cell counts are the counted number of colonies that are developed after a sample has been diluted and spread over the surface of a nutrient medium solidified with agar, contained in a petri dish. As the number of CFU have reduced significantly with increasing silver nanoparticles loadings, therefore, virtually no CFU were observed in the samples containing silver nanoparticles loading of 60 μg/ ml and higher. The bacterial growth inhibition trend found in CFU data has matched well with the results of OD.

Electron Microscopy determined the distribution and location of the silver nanoparticles, as well as the change in morphology of the bacteria after treatment with silver nanoparticles. Silver has been found adhered to the bacterial cells. Bacteria have different membrane structures on the basis of which these are classified as Gram negative or Gram positive. The structural difference lies in the organization of peptidoglycan, which is the key component of membrane structure. Gram-negative bacteria exhibit a thin layer of peptidoglycan (≈2-3 nm) between the cytoplasmic membrane and the outer cell wall. Outer membrane of *E. coli* cells is predominantly constructed from tightly packed lipopolysaccharide (LPS) molecules, which provide an effective permeability barrier [1]. The overall charge of bacterial cells at biological pH values is negative because of excess number of carboxylic groups, which upon dissociation make the cell surface negative. The opposite charges of bacteria and nanoparticles are attributed for their adhesion and bioactivity due to electrostatic forces. It is logical to state that binding of the nanoparticles to the bacteria depends on the surface area available for interaction. Nanoparticles have larger surface area available for interactions which enhances bactericidal effect than the large sized particles; hence they impart cytotoxicity to the microorganisms [14]. The mechanism by which the nanoparticles penetrate into the bacteria is not understood completely, but studies suggest that when *E. coli* was treated with silver, changes took place in its membrane morphology and produced a

significant increase in its permeability affecting proper transport through the plasma membrane, leaving the bacterial cells incapable of properly regulating transport through the plasma membrane, resulting into cell death. It was observed that silver nanoparticles have penetrated inside the bacteria and believed have caused damage by interacting with phosphorus and sulfur containing compounds such as DNA [9]. Silver tends to have a high affinity to react with such compounds. In our study, it is considered that DNA may have lost its replication ability and cellular proteins become inactive after treatment with silver nanoparticles. Another reason would be the release of silver ions from nanoparticles, which will have an additional contribution to the bactericidal efficacy of silver nanoparticles. Heavy metals are toxic and reactive with proteins therefore, they bind protein molecules; as a result cellular metabolism is inhibited causing death of microorganism. High activity of silver nanoparticles is suggested to be due to species difference as they dissolve to release Ag^0 (atomic) and Ag^+ (ionic) clusters, whereas other silver sources such as silver nitrate and silver sulfadiazine release Ag^+ only [6]. It is believed that silver nanoparticles after penetration into the bacteria inactivate their enzymes, generate hydrogen peroxide and cause bacterial cell death [20].

Experimental observations have explained significantly the antibacterial behavior of silver nanoparticles. It is observed in the micrograph shown in figure 6a, that bacterial cells show critical changes and damage in the membrane structure. When *E. coli* was treated with highly reactive metal oxide nanoparticles, an inhibitory effect has taken place [3]. Silver nanoparticles after adherence to the surface of the cell membrane disturbed its respiration as Ag+ interact with enzymes of the respiratory chains of bacteria [21]. It has been observed in our study that a degradation of the membrane structure of *E. coli* has taken place. Metal depletion caused formation of irregular shaped pits in the outer membrane of bacteria which is caused by progressive release of LPS molecules and membrane proteins [22]. In addition, it is believed that silver binds to functional groups of proteins, resulting in protein denaturation [23]. As observed in figure 6.3, bacterial growth log phase has a delayed trend at lower concentrations of silver nanoparticles loadings. Complete bacterial inhibition depends upon the concentrations of silver nanoparticles and on the number of bacterial cells. It reflects that silver nanoparticles have a significant biocide effect in reducing bacterial growth for practical applications.

6.5. References

1. I. Sondi and B. S. Sondi, Journal of Colloid and Interface Science **275,** 177 (2004)
2. J. R. Morones and J. L. Elechiguerra, Nanotechnology **16,** 2346, (2005)
3. P. K. Stoimenov and R. L. Klinger, Langmuir **18,** 6679, (2002)
4. S. H. Jeong and S. Y. Yeo, Materials Science **40**, 5407, (2005)
5. S. L. Percivala and P. G. Bowler, Journal of Hospital Infection **60**, 1, (2005)
6. P. L. Taylor and A. L. Ussher, Biomaterials **26**, 7221, (2005)
7. A. Panacek and A. Kvitek, J. Phys. Chem. B **110**, 16248, (2006)
8. V. Alt and T. Bechert, Biomaterials **25**, 4383, (2004)
9. J. R. Morones, and J. L. Elechiguerra, Nanotechnology **16,** 2346, (2005)
10. C. Lok and C. Ho, Journal of Proteome Research **5**, 916, (2006)
11. A. Oloffs and C. G. Siestrup, Biomaterials **15**, 753, (1994)
12. P. Li and J. Li, Nanotechnology **16**, 1912, (2005)
13. S. Zhang and R. Fu, Carbon **42**, 3209, (2004)
14. C. Baker and A. Pradhan, J. Nanoscience and Nanotechnology **5**, 1, (2004)
15. B. D. Cullity, Elements of X- ray Diffraction, Second Edition, Edison- Wesley Publishing Company, Inc. USA (1978)
16. R. Birringer, Materials Science and Engineering A **117**, 33, (1989)
17. C. G. Granqvisit and R. A. Buharman, J. of Applied Physics **47**, 2200, (1976)
18. F. E. Kruis and H. Fissan, J. Aerosol Sci. **29**, 511, (1998)
19. L. B. Kiss and J. Soderlund, Nanostructured Materials, **12**, 327, (1999)
20. M. Kokkoris and C. C. Trapalis, Nuclear Instruments and Methods in Physics Research B **188**, 67, (2002)
21. K. B. Holt and A. J. Bard, Biochemistry **44,** 13214, (2005)
22. N. A. Amro and L. P. Kotra, Langmuir **16,** 2789, (2000)
23. J. A. Spadaro and T. J. Berger, Antimicrobial Agents and Chemotherapy **6,** 637, (1974)